Journal of Environmental Radioactivity 124 (2013) 74–83

Contents lists available at SciVerse ScienceDirect

Journal of Environmental Radioactivity

journal homepage: www.elsevier.com/locate/jenvrad

Dynamics of soil gas radon concentration in a highly permeable soil based on a long-term high temporal resolution observation series

Katalin Zsuzsanna Szabó [a], Gyozo Jordan [b], Ákos Horváth [c], Csaba Szabó [a,*]

[a] Lithosphere Fluid Research Laboratory, Department of Petrology and Geochemistry, Eötvös University, Pázmány Péter sétány 1/C, 1117 Budapest, Hungary
[b] Institute for Soil Sciences and Agricultural Chemistry, Centre for Agricultural Research, Hungarian Academy of Sciences, Herman Ottó út 15, 1022 Budapest, Hungary
[c] Department of Atomic Physics, Eötvös University, Pázmány Péter sétány 1/A, 1117 Budapest, Hungary

ARTICLE INFO

Article history:
Received 12 November 2012
Received in revised form
11 April 2013
Accepted 12 April 2013
Available online 10 May 2013

Keywords:
Radon gas
Seasonality
Diurnal periodicity
Time series analysis

ABSTRACT

This paper studies the temporal variation of soil gas radon activity concentration in a highly permeable ($k = 2.0E\text{-}11\ m^2$) sandy-gravelly soil in order to understand if temporal variation of soil gas radon activity concentration can affect geogenic radon potential determination. Geogenic radon potential provides information about the potential risk from radon. Its calculation takes into account the equilibrium, saturated at infinite depth, soil gas radon activity concentration (c_∞). This concentration may vary at annual time scale due to the environmental conditions. A long-term (yearly) and high temporal resolution (15 min) observation, applied in this study, reveal various temporal features such as long-term trend, seasonality, daily periodicity and sudden events in soil gas radon time series.

Results show seasonal and daily periodical variation of the measured soil gas radon activity concentration (c_{soilRn}) in a highly permeable sandy-gravelly soil with definite seasons without obvious long transitional periods. The winter (from October 2010 to April 2011) is characterized by 2.5 times higher average soil gas radon activity concentration (median is 7.0 kBq m^{-3}) than the summer (August, September 2010 and May, June, July 2011) (median is 2.8 kBq m^{-3}). Daily periodicity, which is much less than the seasonal one, controls the soil gas radon activity concentration mainly in the summer season. Average (AM) value of c_{soilRn} is higher at night than in the daytime with about 18% and 3.8% in summer and in winter, respectively. As a conclusion, in case of single c_{soilRn} measurement on a highly permeable ($k \geq 2.0E\text{-}11\ m^2$) soil, similar to our test site, c_{soilRn} should be corrected according to the seasons for calculating the equilibrium activity concentration c_∞ value.

1. Introduction

Environmental occurrence of radon gas has been intensively studied in the last decades due to its adverse effects on human health. Its short-lived daughters such as ^{218}Po and ^{214}Po can attach to the aerosols (e.g., dust and cigarette smoke) and can be inhaled into the lung. Deposited radon progenies on the lung bronchi irradiate the cells and can cause tumor (Nazaroff and Nero, 1988).

Radon (^{222}Rn) is a natural radioactive noble gas being one of the daughter elements of ^{238}U. Its direct mother element is radium ^{226}Ra. U-238 and ^{226}Ra are geochemically incompatible lithophile elements, thus they are concentrated in the Earth crust and also can be found in the biosphere (Anderson, 2007). Also, soils, derived from different rock types, contain ^{238}U and ^{226}Ra. The ^{226}Ra constantly produce radon atoms in soil which will enter the soil pore gas via emanation. Radon, generated in soil and rock, can leave the solid grains through three ways: molecular diffusion, direct recoil and molecular diffusion after indirect recoil (Tanner, 1980). Soil radium content and the emanation coefficient determine the effective radium concentration. Radon migration through the soil and rock is affected by molecular diffusion, however it is governed mainly by convection. These processes determine radon activity concentration in soil air (soil gas radon activity concentration) which depends on the depth. The soil gas radon activity concentration increases with depth and exponentially saturates to an equilibrium concentration that is called c_∞ (Nazaroff and Nero, 1988).

Indoor radon concentration is very important since it is responsible for about 50% of the natural radiation dose. Two major factors that determine indoor radon concentration are the entry

* Corresponding author. Tel.: +36 1 372 2500x8338; fax: +36 1 361 2212.
E-mail addresses: sz_k_zs@yahoo.de (K.Z. Szabó), gyozojordan@gmail.com (G. Jordan), akos@ludens.elte.hu (Á. Horváth), cszabo@elte.hu, cszaboo@yahoo.com (C. Szabó).

0265-931X/$ – see front matter © 2013 Elsevier Ltd. All rights reserved.
http://dx.doi.org/10.1016/j.jenvrad.2013.04.004

rate and the ventilation rate. The entry rate appears to be more variable and hence the more important factor in determining houses with high radon levels (Nazaroff and Nero, 1988). It depends on soil gas radon activity concentration, on soil physical characteristics such as permeability, on meteorological circumstances such as temperature and pressure and on building-related factors such as building material and substructure, as well. However, soil and rock are the sources of most of the radon to which people are exposed, whereas the building material, as a second source, can also have significance (Cosma et al., 2013; Nazaroff and Nero, 1988; Righi and Bruzzi, 2006; Szabó et al., 2013).

Modeling and mapping of geogenic and indoor radon potential (RP) provide an opportunity to identify radon-prone areas (Dubois et al., 2010). Therefore, a radon potential map assists to reduce the cumulative radiation risk. Indoor radon potential map shows the actual average health risk in existing houses, whereas geogenic radon potential map reveals potential risk, independently of any existing buildings (Dubois et al., 2010). Geogenic radon potential (GRP) provides information about the source of indoor radon concentration as the major source of indoor radon concentration is the soil gas radon. One method of the calculation of GRP is to estimate a continuous variable from the equilibrium activity concentration (c_∞) of ^{222}Rn in soil gas, in kBq m^{-3} and the effective permeability of soil, in m^2 (k) using the following equation (Neznal et al., 2004).

$$\mathrm{GRP} = \frac{c_\infty}{(-\log_{10}(k) - 10)} \quad (1)$$

In practice, equilibrium activity concentration (c_∞) is generally the ^{222}Rn concentration in soil gas at about 0.8–1 m depth. Parameters used in Eq. (1). can be determined during field work or can be estimated from other available parameters such as ^{226}Ra concentration in dry soil and porosity using transfer functions (Appleton et al., 2011). General measurement depth of soil gas ^{222}Rn concentration (c_{soilRn}) and of corresponding soil permeability is 0.7–1 m (Antonopoulos-Domis et al., 2009; Barnet et al., 2010; Buttafuoco et al., 2010, Castelluccio et al., 2010; Cosma et al., 2010; Dubois, 2005; Gregorič et al., 2010; Gruber et al., 2008; Ielsch and Cushing, 2010; Kemski et al., 2001; Neznal et al., 2010; Pereira and Neves, 2010, Petersell et al., 2005). It is assumed that the measured c_{soilRn} at 0.8 m equal to c_∞, thus its temporal variation should be considered during the evaluation of geogenic radon potential. Several studies show clear temporal variation of c_{soilRn} on a daily or seasonal scale at this depth, depending on the location (Al-Shereideh et al., 2006; Baykut et al., 2010; Crockett et al., 2010; Fujiyoshi et al., 2006, Perrier et al., 2009; Winkler et al., 2001; Zafrir et al., 2012). Perrier et al. (2009) and Crockett et al. (2010) studied the periodic and anomalous phenomena in c_{soilRn} time series and revealed seasonal, diurnal and semi-diurnal components. Baykut et al. (2010) showed daily quasi-periodic component in soil radon data especially during the summer period and they also observed that soil radon is affected by various parameters such as seasonal and daily changes in atmospheric parameters (temperature, pressure, precipitation). Several studies showed the influence of shallow groundwater in particular cases on soil gas radon activity concentration (Pascale Tommasone et al., 2011; Perrier et al., 2009; Przylibski, 2011). As this system is highly complex there is no general description for the c_{soilRn} time dependence.

The principal objective of this study is to determine the dynamics of c_{soilRn} in a highly permeable sandy-gravelly soil and to describe it in terms of trend, periodicity, transient events and autocorrelation. The second goal of this study is to investigate whether the temporal variation of c_{soilRn} influences the geogenic radon potential determination. Robust statistical and time series analysis were used for the characterization of radon dynamics in the studied highly permeable soil. A unique detailed modeling was used to identify and numerically describe long-term cycle and trend components, in addition to periodic changes in c_{soilRn} including seasonal, diurnal or tidal variation.

2. Study area

Soil gas radon activity concentration (c_{soilRn}) has been investigated at a location in the Budapest urban area on the Pest Plane, at the Marczell György Main Observatory of the Hungarian Meteorological Service, (WGS84 N 47°25′43.977″, E 19°10′57.172″) at 137 m a.s.l. (Fig. 1). Hungary has temperate continental climate with a long-term annual average temperature of 11 °C and an average precipitation of 500–550 mm. The underlying rock at the measurement site is Quaternary fluvial sand (Late Pleistocene) (Gyalog, 1996). The sandy-gravelly soil is covered by garden grass at the site. An advantageous feature of the site is that it is a protected area of 10,000 m^2 and it has been undisturbed by human activities for decades. The average groundwater table level is at 10 m depth with open surface. There is a limited (<1 m) groundwater table level fluctuation due to the effect of underground urban structures and the leveling effect of River Danube in distance. Thus, groundwater table fluctuation is assumed to have no influence on temporal variation of soil gas radon activity concentration c_{soilRn} at the site.

The Pannonian Basin in Hungary is largely covered by sediments of various ages (Paleogene, Neogene and Quaternary) and of diverse types (clay, silt, loess, marl, sand, gravel and rock debris) (Gyalog, 1996). Soils, evolved on these sediments, often have high permeability, thus the selected test site located on highly permeable soil is assumed to represent a large area of the Pannonian Basin sediments and soils.

3. Materials and methods

3.1. Field measurements

Soil gas radon activity concentration (c_{soilRn}) was measured in situ with a RAD7 Electronic Radon Detector (Durridge Company Inc., 2000) coupled with soil probe through drying tube from 03 August of 2010 to 22 July of 2011. Inner diameter of the soil probe was ¼ inch. From the soil c_{soilRn} was pumped out from 0.8 m depth (Fig. 1). The instrument settings were “User” protocol, “15 min Cycle“, “Sniff Mode” and “Auto Pump” to collect samples at 15 min cycles, yielding 96 measurements a day. In “Sniff Mode” the device calculates the radon activity concentration from the 3-minute half-life polonium-218 alpha peak at 6.0 MeV and gives radon activity concentration in Bq m^{-3} unit. In “Auto Pump” setting, the pump always switches on for 4 min at the beginning of a new test cycle. If the humidity in the sample cell remains above 10% then the pump stays on to allow the cell to dry out. Then the pump runs for just 1 min in every 5 min until the end of the cycle. The rate of flow of the pump is 1 L min^{-1}. The RAD7 was calibrated in 2009 and the calibration is highly stable according to the manufacturer specifications (Durridge Company Inc, 2000). Typical drift is less than 2% per year. The average uncertainty, expressed by standard deviation, of RAD7 in our measurements was 9.2%. It is about 12% and 7% in case of low (0–5 kBq m^{-3}) and high (5–10 kBq m^{-3}) radon activity concentration values, respectively. In a comparison measurement with the LUK3C scintillation detector of the Babes-Bolyai University, Cluj (Romania) (calibrated in 2010), we found that the two detectors measure the same c_{soilRn} at a 95% confidence level according to a one day comparison test containing 11 measured data. Meteorological parameters (atmospheric air temperature etc.) were measured by Touch Screen Weather Station PCE-FWS 20 (PCE Instruments UK Ltd.). Soil moisture content data was measured by

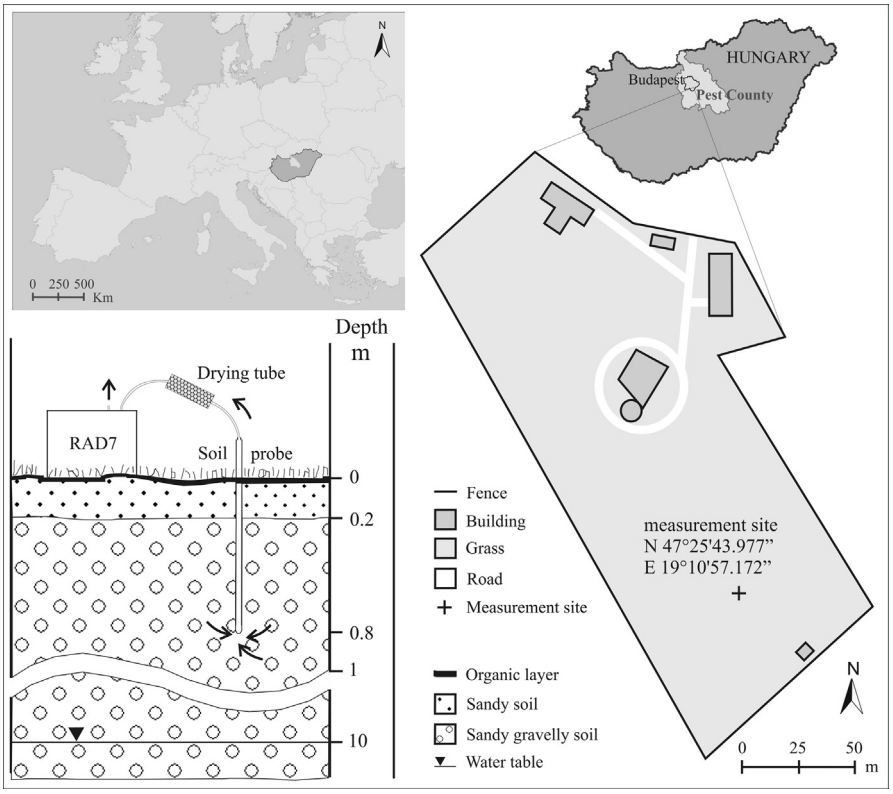

Fig. 1. Map of the measurement site. It is located in the Budapest urban area on the Pest Plane, in the property area of the Marczell György Main Observatory of the Hungarian Meteorological Service, at WGS84 N 47°25′43.977″, E 19°10′57.172″, and 137 m a.s.l.

the Hungarian Meteorological Service Marczell György Main Observatory.

During the measurement period (from 03 August of 2010 to 22 July of 2011) the c_{soilRn} was measured for about one week in every month using 15 min integrating time. Each measurement period was separated by three weeks of no measurement. In August 2010 the measurement period was only three days due to technical limitations. Data series for the observed week in April 2011 has been lost due to unfortunate field conditions. The 15 min sampling time during the observation weeks in each month ('monthly weeks') enabled the capture of high frequency radon activity concentration changes, on one hand, whereas the one year observation period enabled us to capture seasonal changes and long-term trends on the other hand. The permeability of the soil (k, m^2) was measured twice (once in winter and once in summer) at the measurement depth (0.8 m) by Radon-JOK equipment (Radon v.o.s) coupled with the soil probe used for soil gas radon measurement. Permeability of the soil was 2.3E-11 m^2 in August 2010 and 1.7E-11 m^2 in February 2011, yielding 2.0E-11 m^2 average permeability.

3.2. Data processing and data analysis

A time series consists of a set of sequential numeric data taken at equally spaced intervals usually over a period of time or space. We collected 11 so-called "monthly week" datasets which contain measurements at 15 min equidistant intervals for about one week duration (between 3 and 10 days) every month between 03 August 2010 and 22 July 2011. The 11 monthly week datasets altogether represent a year with missing periods between them. In this case the missing values in the unobserved periods were left blank and each monthly week dataset was analyzed separately for the high temporal resolution dynamics (e.g., diurnal). Low-resolution temporal features (e.g., seasonality) were analyzed using the median central values of the 11 monthly week data series.

Summary statistics used in this study include measures of central tendency and variability. These statistics are the minimum, lower quartile, average (arithmetic mean), median, mode, upper quartile, maximum and standard deviation, coefficient of variation, median absolute deviation (MAD), range and inter-quartile range (see Table 1, for example). Variability parameters have an important role since they are particularly suitable for the characterization of changes of a time series (altering variation, called heteroscedasticity, due to seasonal effects in our case). For example, radon exhalation to the open air might be more variable in summer than in winter indicating less topsoil sealing and more dynamic response to surface temperature conditions. Since geochemical data series, such as radon activity concentration measurements, are often characterized by non-normality, heterogeneity and outliers (Jordan et al., 1997; Kurzl, 1988; Reimann et al., 2008), robust statistics like the median for location (central tendency), median absolute deviation (MAD) and the inter-quartile range (IQR) for measure of scale (variability) were used in this study (Hoaglin et al., 1983). The major yearly seasonal period (change in central tendency or location) and the seasonal alteration of variation (change in variability) was described by using the 11 medians and MAD values of the monthly week data series, respectively, and visualized by box-and-whisker plots (see Fig. 5). Extreme variability (i.e. outlying values) was also captured in the plots. An interesting parameter is range/median indicative of total variability containing the outliers, too. In order to account for seasonal differences among the monthly week measurement series, robust variability measures were normalized to the monthly week central values and the monthly week MAD/median relative variability parameters were used for comparison. In this study, IQR/median and MAD/median

Table 1
Summary statistics of the measured soil gas radon activity concentration (c_{soilRn}) data (kBq m^{-3}). Higher and lower populations were separated during statistical analysis and correspond to winter and summer datasets. Winter and summer datasets are separated according to the date. Count is the number of the 15 min measurement periods except in case of winter and summer medians where count means the number of medians of the 6 winter and 5 summer monthly weeks measurements.

Dataset	Count	Minimum	Lower quartile	Median	Upper quartile	Maximum	Average	Standard deviation	MAD	Range	MAD/median
All data (one-year-dataset)	7892	1.01	3.14	5.87	7.03	9.72	5.23	2.10	1.71	8.71	
Higher population	4506	5.00	6.35	6.91	7.41	9.72	6.90	0.86	0.52	4.72	
Lower population	3386	1.01	2.47	2.94	3.57	5.00	3.00	0.80	0.54	3.99	
Winter dataset (Oct 2010–March 2011)	4616	4.18	6.28	6.89	7.40	9.72	6.85	0.91	0.55	5.54	
Summer dataset (Aug–Sep 2010, May–July 2011)	3276	1.01	2.45	2.91	3.50	4.86	2.94	0.75	0.52	3.85	
August (03.08.2010–06.08.2010)	330	1.71	2.42	2.75	3.20	4.02	2.82	0.51	0.36	2.31	0.13
September (03.09.2010–10.09.2010)	675	1.72	2.80	3.39	4.05	4.86	3.40	0.75	0.61	3.14	0.18
October (08.10.2010–18.10.2010)	978	4.18	6.52	6.93	7.34	8.61	6.77	0.89	0.41	4.42	0.06
November (15.11.2010–22.112010)	665	4.97	6.00	6.28	6.68	8.79	6.41	0.61	0.33	3.81	0.05
December (03.12.2010–10.12.2010)	652	5.88	7.00	7.59	8.45	9.72	7.70	0.82	0.70	3.85	0.09
January (04.01.2011–11.01.2011)	660	6.06	6.80	7.05	7.27	8.16	7.04	0.34	0.24	2.10	0.03
February (04.02.2011–14.02.2011)	992	5.77	6.83	7.24	7.68	9.29	7.31	0.67	0.43	3.52	0.06
March (10.03.2011–17.03.2011)	669	4.68	5.33	5.65	5.99	7.41	5.69	0.47	0.33	2.73	0.06
May (04.05.2011–13.05.2011)	859	1.24	2.19	2.53	2.82	3.73	2.49	0.50	0.31	2.49	0.12
June (10.06.2011–17.06.2011)	636	1.62	3.25	3.63	3.84	4.47	3.44	0.61	0.25	2.84	0.07
July (14.07.2011–22.07.2011)	776	1.01	2.19	2.84	3.23	4.05	2.69	0.70	0.47	3.05	0.17
Winter medians	6	5.65	6.28	6.99	7.24	7.59	6.79	0.71	0.43	1.95	
Summer medians	5	2.53	2.75	2.84	3.39	3.63	3.03	0.46	0.31	1.09	

values were found very similar, however IQR/median is systematically higher. Variability of the original monthly week series contains not only the random variations, but also the seasonally dependent amplitude of the diurnal periods, in addition to cycle and trend components. For the pure random component (noise) characterizing system stability, the cycle, trend, periodicity and auto-correlation components have to be removed from the series. Various measures for location and scale were compared to each other using simple least-squares regression analysis. Also, the location dependency of scale was assessed by regression analysis between median and MAD. Summary statistics were calculated for original data series and for the identified sub-populations separately.

Sub-population identification followed the 'natural break' method. A data series, was separated where the cumulative distribution function (CDF) had an inflection point (natural break) identified visually on the cumulative distribution plot (see Fig. 3, e.g.). This point corresponds to a local minimum in the frequency histogram (multi-modal histogram, see Fig. 3, e.g.). Homogeneity test between these sub-populations can reveal similarity between seasons if any. Separation of sub-populations was confirmed at the 95% confidence level by the Mann–Whitney homogeneity test, based on the comparison of medians. Outlying values represent sudden and unusual events, essential for identifying very fast processes such as c_{soilRn} changes due to heavy torrential summer rainfall or gust. Tukey's (1977) inner-fence criteria were used for outlier definition (see Fig. 4, e.g.). All discussed statistical tests, including trend and auto-correlation analyses and homogeneity tests, are significant at the 95% confidence level.

3.3. Time series analysis and modeling

The main assumption of the applied time series analysis is that the high temporal resolution (15 min) sampling frequency is sufficient to describe the sub-weekly diurnal and tidal periods, in addition to sudden changes in c_{soilRn} corresponding to environmental events such as change in temperature and soil moisture content. It is also assumed that the one year dataset enables to describe trend and seasonal periodicity. According to the Nyquist frequency theorem (Makridakis et al., 1998), the studied frequencies should be represented by more than two observation points in each time period. Thus, the highest frequency that can be investigated in our dataset corresponds to 30 min time period, whereas for the one-year dataset the low-frequency sampling component of four weeks can capture temporal features longer than 8 weeks (i.e. two months).

Time series analysis (TSA) defines pattern according to an additive decomposition of the soil gas radon activity measurement series into trend ($T(t)$), cycle ($C(t)$), periodicity ($P(t)$), auto-correlation ($A(t)$), white noise residuals ($\varepsilon(t)$) and events (outliers or transients) ($E(t) = E_O(t) + E_T(t)$) components (Eq. (2)) (Szucs and Jordan, 1994),

$$c(t) = T(t) + C(t) + P(t) + A(t) + E(t) + \varepsilon(t) \quad (2)$$

The additive decomposition was carried out on the 11 equidistant monthly week time series ($c(t)$) separately (Table 1). First, a 5RSSH type nonlinear moving median smoother algorithm was used. This algorithm starts with a 5 point window (i.e. 5×15 min $= 75$ min) moving median calculation then Re-smooth and Split algorithm is applied developed by Tukey (1977). At last it calculates Hanning-type 3 point average (Velleman and Hoaglin, 1981). This process separates the series into 'smooth' ($S_1(t)$) carrying pattern (cycle, trend, periodicity) and 'rough' or 'residual' ($R_1(t)$) containing auto-correlation, noise and outliers, according to Tukey (1977) (Eqs. 3–5),

$$c(t) = S_1(t) + R_1(t), \quad (3)$$

$$S_1(t) = T(t) + C(t) + P(t), \quad (4)$$

$$R_1(t) = A(t) + E(t) + \varepsilon(t). \quad (5)$$

All features or period of time shorter than 75 min (very fast component) join the rough (residuals) eliminating random noise

and the effect of outliers. The residuals are stationary (constant in the mean) and represent the natural variability of soil gas radon, in addition to the stochastic and the sampling uncertainties.

First, the above obtained 'rough' ($R_1(t)$) is processed and outliers are defined by the previously described inner-fence criteria and subsequently removed. The outlier-free series is then subject to tests for randomness of median, sign and Box–Pierce tests to check if no pattern remains in the noise as trend, periodicity and auto-correlation, respectively. In this study all residual series were found random at the 95% confidence level. A detailed auto-correlation analysis is performed to identify the autoregressive property in the outlier free residual series ($R_1(t)$) and to describe the 'memory effect', inertia or the predictability of the soil gas radon system. In this study no auto-correlation significant at the 95% was found, which means that the observed soil radon is highly variable and there is no relationship among the successive soil gas radon activity concentrations at the 15 min time scale. Finally, the statistical distribution of the outlier-free noise is described by the above mentioned summary statistics.

Second, the 'smooth' ($S_1(t)$) is processed to model trend, cycle and periodicity. In order to describe the 96 samples long ($24 \times 4 = 96$; 1 h equals four 15 min periods) diurnal period in the 5RSSH smoothed data, it was made stationary by removing the cycle and trend components with a 101 (>96) data moving average smoother. In this way the 5RSSH 'smooth' ($S_1(t)$) was further separated into another smooth containing the cycle and trend components ($S_2(t)$) and another rough containing the diurnal (and less than one week-long) periodicity ($R_2(t)$) (Eqs. 6–8),

$$S_1(t) = S_2(t) + R_2(t), \tag{6}$$

$$S_2(t) = T(t) + C(t), \tag{7}$$

$$R_2(t) = P(t). \tag{8}$$

Periodicity was analyzed by the periodogram showing the power at each Fourier frequency (see Fig. 6B). The periodogram shows the data in the frequency domain by considering how much variability exists at different frequencies. Once the frequencies in the data were identified, periodicity was modeled with sine waves fit to each monthly week data series with the least-squares method. The best fit was indicated by the smallest root-mean-square error (RMSE) value. The amplitude of the calculated sine waves may reveal seasonal differences. From the 101 moving average smoothed data, the trend component was modeled by a simple linear least-squares regression line to $S_2(t)$ (see Fig. 6A). After subtracting the trend line from the smoothed series, the pure cycle component ($C(t)$) is obtained (see Fig. 6A).

4. Results and discussion

4.1. Statistical analysis

Fig. 2 shows the observed 11 monthly week data series. The altogether 7892 observed c_{soilRn} data have a median 5.87 kBq m^{-3}, average 5.23 kBq m^{-3} with a 2.10 kBq m^{-3} standard deviation (Table 1). The standardized skewness and kurtosis are out of the −2 to +2 range indicating non-normality in the data. No outliers are obvious however the distribution has a strong bimodal character (Fig. 3). We separated the distribution at 5.00 kBq m^{-3} (lower part ≤ 5.00 kBq m^{-3}) at the major natural break (inflexion point) in the cumulative distribution function (CDF) plot corresponding to the local minimum in the histogram (Fig. 3). The lower population has a median 2.94 kBq m^{-3}, average of 3.00 kBq m^{-3} and standard deviation 0.80 kBq m^{-3} and the higher population has a median 6.91 kBq m^{-3}, average of 6.90 kBq m^{-3} and standard deviation 0.86 kBq m^{-3} corresponding to summer and winter seasons, respectively. Summary statistics of these populations are shown in Table 1. In the lower (summer) population there are no outliers, whereas in the higher (winter) population there are 48 outliers (Fig. 3). From these, 42 outliers are in December and 6 outliers are in February. The robust Mann–Whitney Test has confirmed the statistically significant separation of the populations at the 95% confidence level. The higher and the lower sub-populations correspond to the summer and winter seasons comprising the months August, September, May, June, July and October, November, December, January, February, March, respectively (Fig. 3).

If we separate the dataset according to the dates, when the data from August 2010 to September 2010 and from May 2011 to July 2011 is called summer dataset and data from October 2010 to March 2011 is called winter dataset, we obtain almost the same results. Summer median is 2.91 kBq m^{-3}, average is 2.94 kBq m^{-3}, and standard deviation is 0.75 kBq m^{-3}, winter median is 6.89 kBq m^{-3}, average is 6.85 kBq m^{-3} and standard deviation is 0.91 kBq m^{-3} (Table 1). This confirms seasonality in c_{soilRn} at this site.

The monthly week datasets were also found heterogeneous with multi-modal distribution and several outliers. The sub-populations were identified, separated and compared in the way described above. An example is shown for June 2011 in Fig. 4. Proportion of the outliers in the monthly week datasets decreased in the order of 17% in June 2011, 13% in October 2010, 6% in November 2010, 2% in February 2011 and 1% in March 2011. No

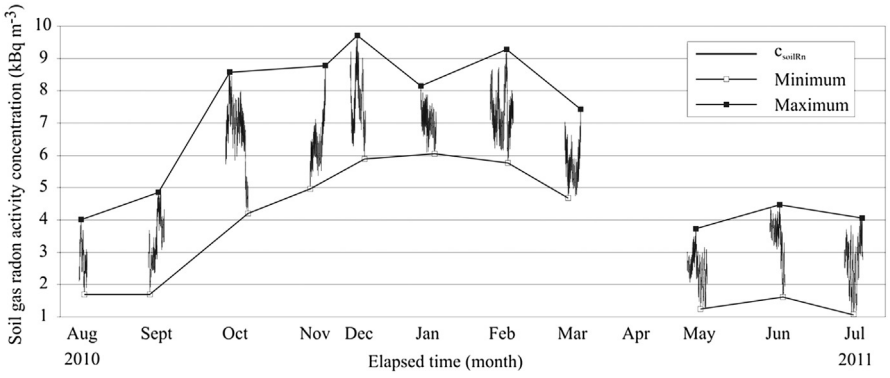

Fig. 2. Times series of the observed 11 monthly week soil gas radon activity concentration (c_{soilRn}) data (from 03 August 2010 to 22 July 2011) and the minimum and maximum values which show the range of each monthly week dataset.

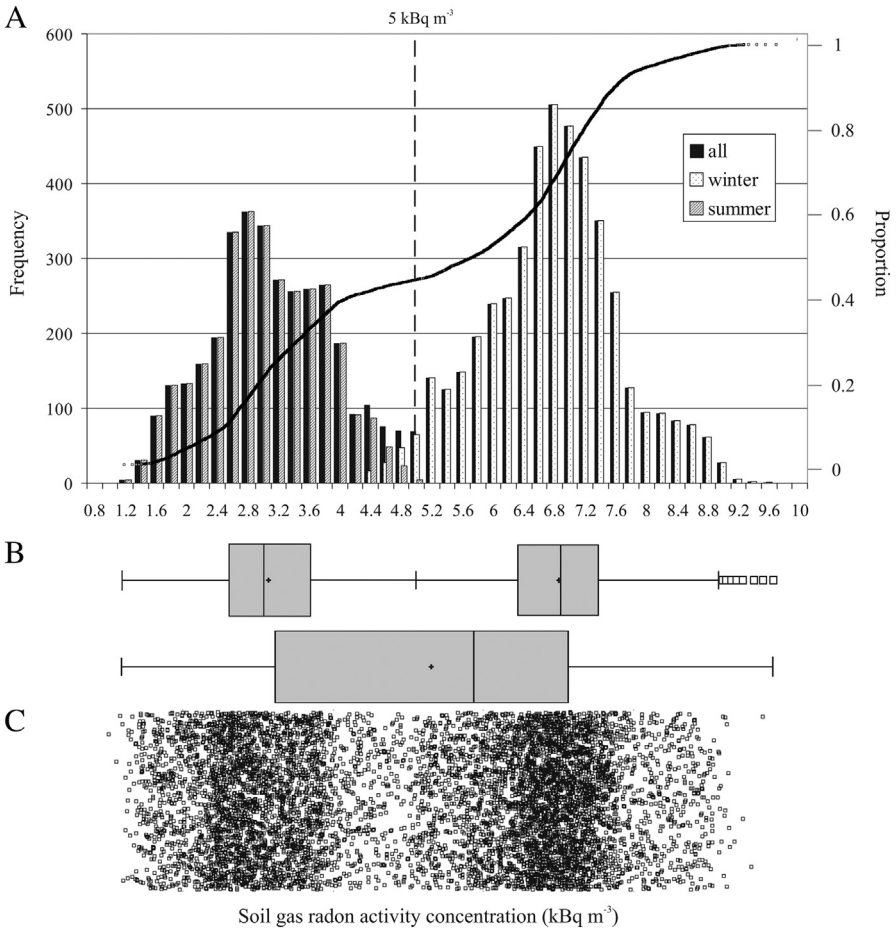

Fig. 3. Histogram, quantile plot (A), box-and-whisker plot (B) and scatterplot (C) of the observed soil gas radon activity concentration (c_{soilRn}) dataset of the one year period (from 03 August 2010 to 22 July 2011). Dashed line shows the 5 kBq m^{-3} separating the one year dataset. Box-and-whisker plots below the histogram show the identified sub-populations, too.

outliers were found in August, September, December 2010 and January, May, July 2011. Summary statistics of the monthly week datasets, representing the different months, is also shown in Table 1. Box-and-whisker plot of the monthly week datasets from August 2010 to July 2011 shows a clear separation of the summer and winter seasons on the monthly basis (Fig. 5). Again, lower soil gas radon activity concentrations were detected in August, September 2010 and in May, June, July 2011 in the summer period, and higher activity concentrations were found in October, November, December 2010 and in January, February, March 2011 in the winter period. When the medians of the monthly week datasets are aggregated into two groups (5 summer months and 6 winter months), the hence obtained two groups' medians (2.84 kBq m^{-3} and 6.99 kBq m^{-3}) are statistically significantly different according to the Mann–Whitney Test.

When the maximum (extreme) seasonal variability measured by the 5 and 6 (seasonal summer and winter) range parameters are compared similarly, no significant difference is found. Similarly, no significant difference was observed between the two major seasons' (summer and winter) MAD values indicating that the absolute variability of measured c_{soilRn} of the two seasons are similar. These results suggest the strong seasonality in c_{soilRn} data in the central or overall radon during the studied year, whereas the extreme variations are similar. Higher soil gas radon activity concentration does not suggest higher variation in the studied soil system.

It is interesting to see how many of the successive monthly weeks represented months are similar or homogeneous. Since the successive observed monthly week data are heterogeneous inside, the identified 28 sub-populations were compared to each other. Nine of the 28 monthly week sub-populations were excluded because they did not have the minimum number of samples ($8\leq$) needed for the Mann–Whitney Test. There is no statistically significant difference between the medians of August 2010–May 2011 (main sub-populations) May 2011–June 2011 (minor_high and main sub-populations) in summer, and between October 2010–January 2011 (main sub-populations) in winter (Fig. 5). This means that the c_{soilRn} values in the summer period and in the winter period are more similar to each other than between the seasons.

This result confirms the strong seasonality of soil gas radon activity concentrations (c_{soilRn}) during the studied year and the separation of seasons is sharp and definite without obvious long transitional periods. This suggests the existence of threshold values of control parameters separating high and low c_{soilRn}.

There are similarities in the time dependence of radon concentration in caves and in permeable soils, and there are differences, as well. Radon activity concentration dynamics (some weeks long rapid transition period between seasons) has already been described in caves, cellars, etc. (Duenas et al., 2011; Fijalkowska-Lichwa and Przylibski, 2011; Hakl et al., 1996, 1997; Hunyadi et al., 1991; Nagy et al., 2012; Przylibski, 1999). In these underground structures temperature induced atmospheric

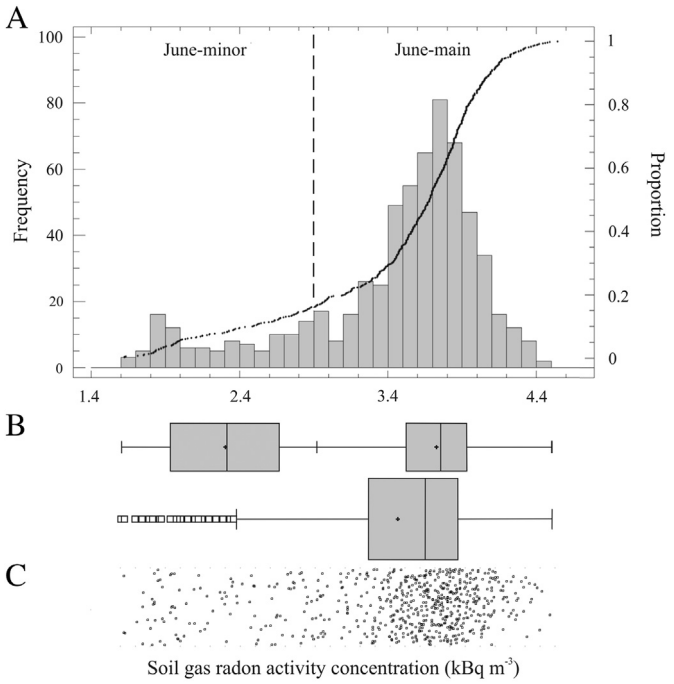

Fig. 4. Histogram, quantile plot (A), box-and-whisker plot (B) and scatterplot (C) of the observed soil gas radon activity concentration (c_{soilRn}) dataset of June 2011. Box-and-whisker plots below the histogram show the identified sub-populations, too.

pressure differences govern the natural air exchange, thus the dynamics of radon concentration also will be changed. In caves, generally, higher air radon activity concentrations are in summer, in contrary, in the soil higher radon activity concentrations occurs generally in winter in the soil, which is the opposite to the caves. Reason of the cave dynamics is that in the cave air convection starts inwards when the mean temperature of cave air exceeds the external atmospheric temperature in winter time. In this way the radon depleted external air dilutes the internal air with elevated radon activity concentration by moving inward the cave. In summer, when the atmospheric temperature rises above mean internal cave air temperature, the direction of the air flow changes to the opposite way. The colder air in the cave is more dense than the external air, thus the air flows out of the cave through the entrance. The air balance is recovered through the radon rich fracture system giving account for the summer maxima (Hunyadi et al., 1991).

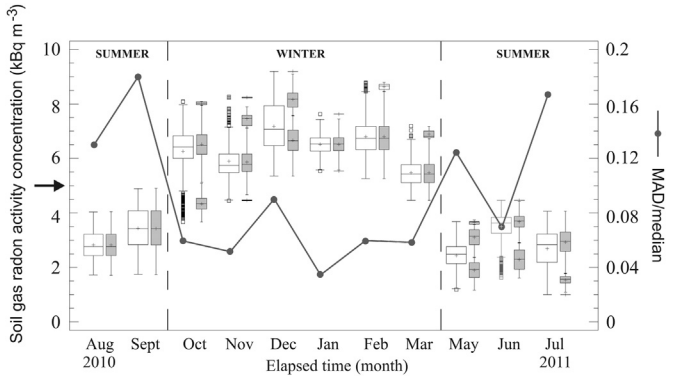

Fig. 5. Box-and-whisker plot of the original monthly week soil gas radon activity concentration (c_{soilRn}) data series (empty box) and the identified 28 sub-populations (grey plots). Main population is the population with the most observations of a monthly week, minor population is separated from the main population and it can be high or low according to the values. Vertical dashed lines separate the seasons. Black arrow on the ordinate indicates the natural break (inflexion point) at 5 kBq m^{-3} c_{soilRn} separating summer and winter seasons on statistical basis. Points connected by solid line show the MAD/median monthly week relative variations.

In most cases, caves and cellars are approximately horizontally embedded in a rock formation having one or more large, relatively high-lying entrance hole to the open air. The soil-air system is different from geometric point of view since it is a vertical system and connects to the open air in a different way. In summer, soil gas radon can easily move in the dry, cracked, porous soil and can exhale to the open air, whereas in winter the soil is sealed by snow and frozen uppermost soil layer and radon cannot exhale out to the open air. Additionally, the higher soil moisture content in winter cause not only higher radon emanation, but also higher soil gas radon activity concentration (Nazaroff and Nero, 1988). The day–night radon differences are due to the dynamics of turbulent diffusion. At a windless night a stable temperature inversion forms and stops the turbulent diffusion in the boundary layer. In this case the soil radon flux is reduced and the soil gas radon concentration rises up. After the sunrise this stable system vanishes and the turbulent diffusion starts yielding increased radon flux from the soil (Kumar et al., 1999).

During our measurement period the average atmospheric temperature at the site was 12.4 °C with an average of 19.2 °C in summer and 5.7 °C in winter. The average soil moisture content was 81.6% with an average of 61.6% in summer and 93.5% in winter. The reason for the strong seasonality of c_{soilRn} is the seasonal change of temperature and humidity (Iakovleva and Ryzhakova, 2003; Sundal et al., 2008).

Soil gas radon activity concentration is a necessary quantity for assessing the geogenic radon potential as described above (Eq. (1)). Generally, it is determined by a single measurement from one season. The 2.5 times difference in c_{soilRn} between the seasons at this highly permeable site is large enough to obtain significant difference of GRP. In the widely used classification methods of Neznal et al. (2004) and Kemski et al. (2001) this significant difference may result in different GRP categories. In order to avoid misclassification, the measured c_{soilRn} should be corrected to get the annual average equilibrium concentration c_∞ value according to the seasons at this highly permeable site.

Since highly permeable soils dominate certain regions, for instance, on different age and type sediments as shown previously, this seasonal phenomenon is necessary to be taken into account during regional geogenic radon potential mapping in Hungary.

4.2. Long-term change: variability at different seasons

According to the relative MAD/median measure of variability of the monthly week datasets, the highest data scatter occurs in August and September in 2010 and in May, June, July in 2011 (Fig. 5). These are the summer months identified above. A likely reason for this is the extreme change in soil parameter values and daily temperature changes. Consistently, the overall relative variability is low in winter months, except for December 2010. Maximum scatter in the data based on range/median measure of variability, which is sensitive to the effect of extreme values, also occurs in the summer period, except for June 2010. Again, the weather conditions impacting soil characteristics such as soil temperature, wetness and pore gas pressure are more variable in summer, often associated with extreme events of sudden temperature variations (Sundal et al., 2008; Smetanová et al., 2010). The average relative variability (median of the monthly weeks' MAD/median values) is 13% and 6% for the summer and winter periods, respectively.

It is interesting that there is no obvious transition between the two seasons and the soil radon activity concentration changes from one state to the other both in terms of the seasonal level (median value) and of the variability (MAD/median) (Fig. 5). This indicates that soil radon is controlled by a factor(s) with definite threshold(s).

4.3. Long-term change: trend and cycle

In order to study long-term trend in the c_{soilRn} data, trend analysis was carried out for the whole one year data where the original monthly week data series were replaced by their 11 median values. Similarly, trend was fit separately to the seasons. With respect to temporal scales beyond the seasonal (half year) period, there is no obvious long-term pattern according to trend analysis with 95% confidence.

The 11 monthly week data series were also studied separately and a simple linear regression line was fit to the data series denoised with a 5RSSH smooth and subsequently treated with a 101 moving average smooth to remove diurnal (96 sample-long and shorter) periodicity ($S_2(t)$). The success of the smooth was confirmed by the observed lack of any periodicity in the smoothed series by Fourier and auto-correlation analysis.

The removal of trend form the treated series reveals the cycle component ($C(t)$). All the monthly week data series cycles have two equidistantly located local minima and maxima indicating a half-week periodicity (Fig. 6A). This was confirmed by the periodograms showing significant 2.5–3 days periodicity in the cycle.

No significant trend was found in December 2010, February, March and July 2011, whereas variable positive (September and November 2010) and negative (August, October 2010, January, May, June 2011) trends with various strong correlation was found ranging from the weakest (0.51) in November 2010 to the strongest (−0.97) in August 2010. An example for trend modeling and cycle identification is shown in Fig. 6A for December 2010. These local trends do not represent the trend for the whole months.

4.4. Short-term change: diurnal periodicity

In the second 'rough' ($R_2(t)$), remaining after the 5RSSH and 101 moving average smoothes, significant diurnal periodicity was found in all the 11 monthly week data series with an average 93 data point lengths (0.97 day frequency) (Fig. 6B). In order to numerically model diurnal periodicity and to check for possible seasonal variations, the obtained diurnal sine waves were fitted with the least-squares method (Makridakis et al., 1998) (Fig. 6C and D). The best fit to the data was defined by the minimum value of the root mean square error (RMSE). Daily period in the 11 monthly week data series ranged between 90 and 99 data points corresponding to 0.94 day and 1.03 day, the average period was 95 equaling one day. In summer, wave length is more constant but it is highly variable in winter (Fig. 6C and D). However, the average amplitude was found 0.3 kBq m^{-3}, it was twice higher in summer (0.4 kBq m^{-3}) than in winter (0.2 kBq m^{-3}) (Fig. 6C and D). Again, besides the random variability, this shows a higher and more

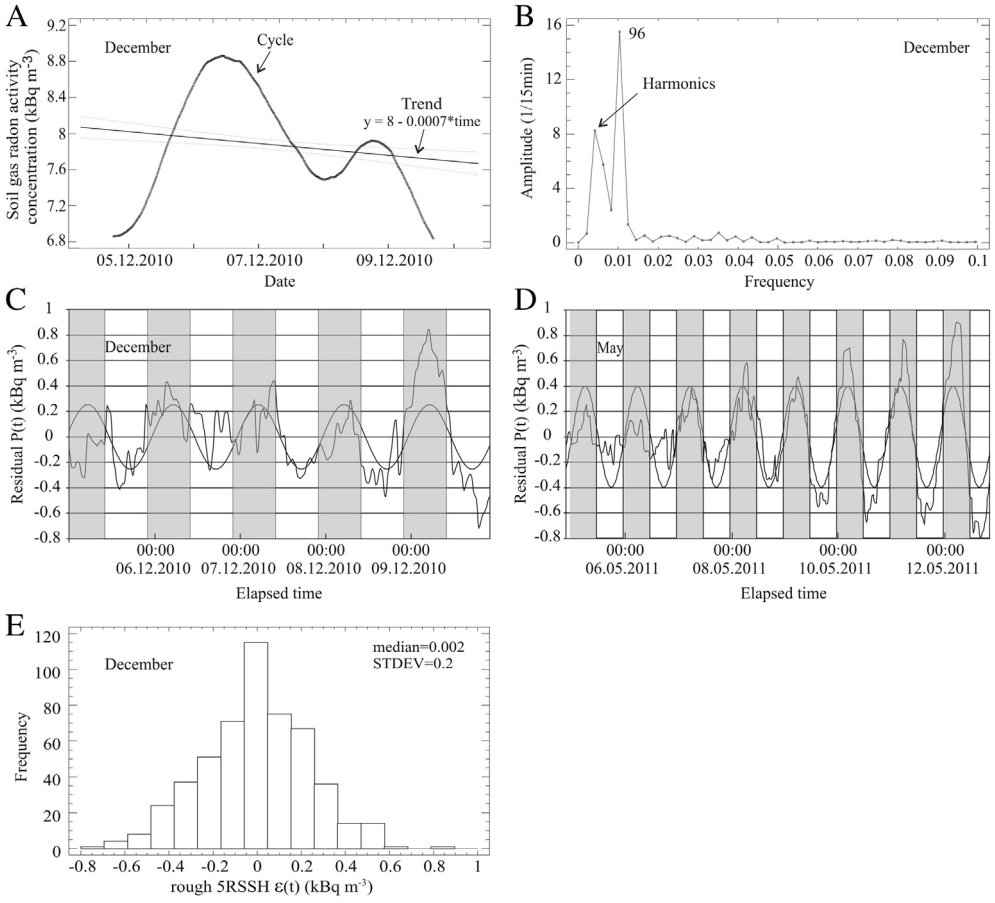

Fig. 6. A: Trend and cycle modeling in smooth of $S_2(t)$ (5RSSH and SMA101 smoothed) soil gas radon activity concentration (c_{soilRn}) dataset for December 2010., B: periodogram of the rough of $S_2(t)$ (5RSSH and SMA101 smoothed) soil gas radon activity concentration (c_{soilRn}) dataset for December 2010. It shows the period of time (96) equal to one day and a harmonics., C: fitted diurnal sine wave to the P(t) for December 2010. Transparent black rectangles show nights from 22:00 to 10:00., D: fitted diurnal sine wave to the P(t) for May 2011. Transparent grey rectangles show nights from 22:00 to 10:00., E: $R_1(t)$ (rough of the 5RSSH smooth) of December 2010 dataset shows the noise.

regular systematic (diurnal) variation in summer than in winter and most likely driven by the climatic and soil conditions (Baykut et al., 2010). Daily periodicity shows higher c_{soilRn} at night from about evening 20:00–24:00 to about morning 07:00–10:00 and lower in the daytime also in summer, as well as in winter. Average c_{soilRn} are higher at night than in the daytime with about 18% and 3.8% in summer and in winter, respectively. Considering the uncertainty of a single measurement this difference is significant in summer, whereas in winter it is negligible.

4.5. Short-term change: outliers and transients

An interesting transient feature, occasionally occurring, is that higher c_{soilRn} values were found in the daytime and lower at night on 7. September 2010, on 5. December 2010, on 11. February 2011 and on 16. March 2011 based on the calculated average c_{soilRn} at night (from 22:00 pm to 10:00 am) and in the daytime (from 10:00 am to 22:00 pm) for every day (Fig. 6C, for example on 5. December 2010). This is opposite behavior than daily periodicity described above (Fig. 6C and D). All these events were during upward trend of the monthly week time series of c_{soilRn}.

We found no pattern (trend, periodicity, auto-correlation) among the outliers in the first 'rough' ($R_1(t)$) (residuals after the 5RSSH smooth, the ε random noise component). Outliers occurred any times of day. Sudden events in c_{soilRn} are most probably associated with climatic events of torrential rainfall or wind storms.

An interesting transient phenomenon is that there is amplitude and frequency differences between the c_{soilRn} and the sine wave fitted to the smoothed monthly week series. Fig. 6C and D show the $P(t)$ and the fitted sine wave for December 2010 and May 2011. There are high deviations both in the frequency and amplitude during winter months, however c_{soilRn} time series are well-behaved and fit much better the regular sine wave during the summer months.

No interpretable auto-correlation was found in the outlier-free 11 monthly weeks noise (ε) (5RSSH rough) data series ($R_1(t)$). Although correlation was found in all series at the second time lag significant at the 95% confidence level, but all were very small between $r = 0.3$ and $r = -0.2$. This indicates the high variability of soil gas radon and the lack of relationship between successive measurements taken at the 15 min intervals.

The outlier-free first rough ($R_1(t)$) for the 11 monthly week time series, the noise component, had a zero average and median (at the 95% confidence level) with homogeneous and symmetric distribution (Fig. 6E). Summary statistics clearly show that the stochastic variability of the c_{soilRn} is significantly higher in winter than in summer as confirmed by the F Test with the 95% confidence.

5. Conclusions

Long-term high temporal resolution soil gas radon activity measurement series could capture the seasonal and diurnal variation of c_{soilRn} on the studied highly permeable (k = 2.0E-11 m^2) sandy-gravelly soil developed on fluvial sand at temperate continental climate. Clear seasonality characterizes the one-year measurement series at the studied site, but it would be further confirmed by multi-annual measurement series at the site. The c_{soilRn} is about 2.5 times higher in winter (median is 7.0 kBq m^{-3}) than in summer (median is 2.8 kBq m^{-3}). The reason for the strong seasonality of c_{soilRn} is the seasonal change of temperature and humidity. Therefore, the measured c_{soilRn} should be corrected to obtain the annual average equilibrium concentration c_∞ value according to the seasons at this highly permeable site.

The difference of the minimum and maximum values (range) for months do not change. Thus meteorological and pedologic circumstances cause simply a shift of the average c_{soilRn} and do not result in seasonally different extreme values.

Relative variability, including the extreme values (range/median) changes, being higher in summer than in winter. Thus, winter c_{soilRn} is more accurately determinable by a single measurement than summer c_{soilRn}. Also, due to the threshold effect, c_{soilRn} is highly characteristic to the seasons.

The average relative variability (MAD/median) is also seasonally dependent. It is higher in summer (13%) than in winter (6%). Reason for this is that the soil-radon system is primarily driven by surface weather conditions being more extreme in summer than in winter. The sealing effect of the wet and frozen uppermost organic-rich soil horizon adds to complexity of the underground system and contributes to the moderate radon atmospheric emission in winter. Finally, the overall drying and opening of soil cracks and the pore space in the hot summer period also promotes the influence of atmospheric conditions. As a conclusion heteroscedasticity characterizes the c_{soilRn} time series since the variability is not time invariant.

Soil gas radon activity concentration has a demonstrated average periodicity of one day throughout the year irrespective to the seasons. Average c_{soilRn} was also higher at night than in daytime with about 18% and 3.8% in summer and in winter, respectively. This difference is much less than the seasonal one. The c_{soilRn} depletion in the warm periods both in summer and the daylight period suggests that soil radon is lost from the observed soil pore space to the atmosphere due to the upward gas flow and the increased diffusion coefficient of radon gas. In the cold, more wet and probably more sealed by the top organic-rich layer winter soil conditions radon tends to stay in the soil pore space, its concentration is less influenced by the surface conditions.

Detailed soil radon time series analysis shows that measured soil radon activity concentrations are highly dependent on the season and much less on the diurnal period. These results have fundamental implications to spatial soil radon mapping and determination of radon potential of a building site suggesting a very careful sampling design.

Acknowledgment

The authors thank József Nagy and Zoltán Nagy, Hungarian Meteorological Service, Marczell György Main Observatory for enable the measurements and provide soil moisture content data. Thanks also go to Tadeusz A. Przylibski and to the other two anonym referees and the associate editor Paul Martin, for their useful comments and suggestions. The authors give special thank to Botond Papp and Cosma Constantin, Babes-Bolyai University, Cluj (Romania) for the soil gas radon comparison measurement. The research has been founded by the Doctoral School for Environmental Sciences, Eötvös University (Budapest), by the TÁMOP-4.2.2/B-10/1-2010-0030 (Individual steps on the way of scientific research) Project and supported by the European Union and Hungary in the framework of the TÁMOP 4.2.4.A/1-11-1-2012-0001 "National Excellence Program – National Program for elaboration and run a system for personal support for Hungarian students and researchers".

This is the 54th publication of the Lithosphere Fluid Research Laboratory (LRG) at Eötvös University.

References

Al-Shereideh, S.A., Bataina, B.A., Ershaidat, N.M., 2006. Seasonal variations and depth dependence of soil radon concentration levels in different geological formations in DeirAbu-Said district, Irbid – Jordan. Radiat. Meas. 41, 703–707.

Anderson, D.L., 2007. New Theory of the Earth, first ed. Cambridge University Press, New York.

Antonopoulos-Domis, M., Xanthos, S., Clouvas, A., Alifrangis, D., 2009. Experimental and theoretical study of radon distribution in soil. Health Phys. 97, 322–331.
Appleton, J.D., Doyle, E.R., Fenton, D., Organo, C., 2011. Radon potential mapping of the Tralee-Castleisland and Cavan areas (Ireland) based on airborne gamma-ray spectrometry and geology. J. Radiol. Prot. 31, 221–235.
Barnet, I., Pacherová, P., Preusse, W., Stec, B., 2010. Cross-border radon index map 1: 100 000 Lausitz – Jizera – Karkonosze – region (northern part of the Bohemian Massif). J. Environ. Radioactiv. 101, 809–812.
Baykut, S., Akgül, T., Inan, S., Seyis, C., 2010. Observation and removal of daily quasi-periodic components in soil radon data. Radiat. Meas. 45, 872–879.
Buttafuoco, G., Tallarico, A., Falcone, G., Guagliardi, I., 2010. A geostatistical approach for mapping and uncertainty assessment of geogenic radon gas in soil in an area of southern Italy. Environ. Earth Sci. 61, 491–505.
Castelluccio, M., Moroni, M., Tuccimei, P., Neznal, M., Neznal, M., 2010. Soil gas radon concentration and permeability at "Valle della Caffarella" test site (Roma, Italy). Evaluation of gas sampling techniques and radon measurements using different approaches. In: Barnet, I., Neznal, M., Pacherova, P. (Eds.), Proc., 10th International Workshop on the Geological Aspects of Radon Risk Mapping. Czech geological survey, Radon v.o.s., Prague, pp. 61–71.
Cosma, C., Papp, B., Nita, D.C., Dinu, A., Sainz, C., 2010. Soil radon measurements in radon prone area Stei-Baita (Romania). In: Barnet, I., Neznal, M., Pacherova, P. (Eds.), Proc., 10th International Workshop on the Geological Aspects of Radon Risk Mapping. Czech geological survey, Radon v.o.s., Prague.
Cosma, C., Cucos-Dinu, A., Papp, B., Begy, R., Sainz, C., 2013. Soil and building material as main sources of indoor radon in Baita-Stei radon prone area (Romania). J. Environ. Radioactiv. 116, 174–179.
Crockett, R.G.M., Perrier, F., Richon, P., 2010. Spectral-decomposition techniques for the identification of periodic and anomalous phenomena in radon time-series. Nat. Hazard. Earth Sys. 10, 559–564.
Dubois, G., 2005. EUR 21892 EN – an Overview of Radon Surveys in Europe, Office for Official Publication of the European Communities.
Dubois, G., Bossew, P., Tollefsen, T., De Cort, M., 2010. First steps towards a European atlas of natural radiation: status of the European indoor radon map. J. Environ. Radioactiv. 101, 786–798.
Dueñas, C., Fernández, M.C., Cañete, S., Pérez, M., Gordo, E., 2011. Seasonal variations of radon and the radiation exposure levels in Nerja cave. Spain. Radiat. Meas. 46, 1181–1186.
Durridge Company Inc. RAD7 Electronic Radon Detector, 2000. User Manual.
Fijalkowska-Lichwa, L., Przylibski, T.A., 2011. Short-term ^{222}Rn activity concentration changes in underground spaces with limited air exchange with the atmosphere. Nat. Hazard. Earth Sys. 11, 1179–1188.
Fujiyoshi, R., Sakamoto, K., Imanishi, T., Sumiyoshi, T., Sawamura, S., Vaupotic, J., Kobal, I., 2006. Meteorological parameters contributing to variability in ^{222}Rn activity concentrations in soil gas at a site in Sapporo, Japan. Sci. Total Environ. 370, 224–234.
Gregorič, A., Žvab, P., Vaupotič, J., Mazur, J., Kozak, K., 2010. Radon levels in outdoor air and soil gas related to geology of Slovenia. In: Barnet, I., Neznal, M., Pacherova, P. (Eds.), Proc., 10th International Workshop on the Geological Aspects of Radon Risk Mapping. Czech geological survey, Radon v.o.s., Prague. http://www.radon.eu/workshop2010/pres/vaupotic.pdf.
Gruber, V., Baumgartner, A., Seidel, C., Maringer, F.J., 2008. Radon risk in Alpine regions in Austria: risk assessment as a settlement planning strategy. Radiat. Prot. Dosim. 130, 88–91.
Gyalog, L. (Ed.), 1996. Signal Code of the Geological Maps and Short Description of the Stratigraphical Units I (in Hungarian). Geological Institute of Hungary, Budapest. Special Paper 187.
Hakl, J., Csige, I., Hunyadi, I., Várhegyi, A., Géczy, G., 1996. Radon transport in fractured porous media-experimental study in caves. Environ. Int. 22, 433–437.
Hakl, J., Hunyadi, I., Csige, I., Géczy, G., Lénárt, L., Várhegyi, A., 1997. Radon transport phenomena studied in karst caves – international experiences on radon levels and exposures. Radiat. Meas. 28, 675–684.
Nagy, H.É., Szabó, Z., Jordán, G., Szabó, C., Horváth, Á., Kiss, A., 2012. Time variations of ^{222}Rn concentration and air exchange rates in a Hungarian cave. Isot Environ. Health Stud. 48, 1–9.
Hoaglin, D.C., Mosteller, F., Tukey, J.W., 1983. Understanding Robust and Exploratory Data Analysis. John Wiley and Sons Inc., New York.
Hunyadi, I., Hakl, J., Lenart, L., Géczy, G., Csige, I., 1991. Regular subsurface radon measurements in Hungarian karstic regions. Nucl. Tracks Radiat. Meas. 19, 321–326.
Iakovleva, V.S., Ryzhakova, N.K., 2003. Spatial and temporal variations of radon concentration in soil air. Radiat. Meas. 36, 385–388.
Ielsch, G., Cushing, M.E., Combes, Ph., Cuney, M., 2010. Mapping of the geogenic radon potential in France to improve radon risk management: methodology and first applications to region Bourgogne. J. Environ. Radioactiv. 101, 813–820.
Jordan, G., Szucs, A., Qvarfort, U., Szekely, B., 1997. Evaluation of metal retention in a wetland receiving acid mine drainage. In: Xuejin, Xie (Ed.), Proceedings, IGC 30, Geochemistry 19, pp. 189–206.
Kemski, J., Siehl, A., Stegemann, R., Valdivia-Manchego, M., 2001. Mapping the geogenic radon potential in Germany. Sci. Total Environ. 272, 217–230.
Kumar, A.V., Sitaraman, V., Oza, R.B., Krishnamoorthy, T.M., 1999. Application of a numerical model for the planetary boundary layer to the vertical distribution of radon and its daughter products. Atmos. Environ. 33, 4717–4726.
Kurzl, H., 1988. Exploratory data analysis: recent advances for the interpretation of geochemical data. J. Geochem. Explor. 30, 309–322.
Makridakis, S.G., Wheelwright, S.C., Hyndman, R.J., 1998. Forecasting: Methods and Applications, third ed. Whiley Publisher, New York.
Nazaroff, W.W., Nero Jr., A.V., 1988. Radon and Its Decay Products in Indoor Air, United States of America. John Wiley & Sons.
Neznal, M., Neznal, M., Matolin, M., Barnet, I., Miksova, J., 2004. The New Method for Assessing the Radon Risk of Building Sites. Czech Geol. Survey, Prague. Czech Geol. Survey Special Papers no. 16. http://www.radon-vos.cz/pdf/metodika.pdf.
Neznal, M., Neznal, M., Barnet, I., 2010. Practical usefulness of radon risk maps and detailed in-situ classification of radon risk. Nukleonika 55, 471–475.
Pascale Tommasone, F., De Francesco, S., Cuoco, E., Verrengia, G., Santoro, D., Tedesco, D., 2011. Radon hazard in shallow groundwaters II: dry season fracture drainage and alluvial fan upwelling. Sci. Total Environ. 409, 3352–3363.
Pereira, A.J.S.C., Neves, L.J.P.F., 2010. Geogenic controls of indoor radon in Western Iberia. In: Barnet, I., Neznal, M., Pacherova, P. (Eds.), Proc., 10th International Workshop on the Geological Aspects of Radon Risk Mapping. Czech Geological Survey. Radon v.o.s., Prague, pp. 205–210. http://www.radon.eu/workshop2010/pres/neves.pdf.
Perrier, F., Richon, P., Sabroux J-, C., 2009. Temporal variations of radon concentration in the saturated soil of Alpine grassland: the role of groundwater flow. Sci. Total Environ. 407, 2361–2371.
Petersell, V., Åkerblom, G., Ek, B.M., Enel, M., Möttus, V., Täht, K., 2005. Radon Risk Map of Estonia: Explanatory Text to the Radon Risk Map Set of Estonia at Scale of 1:500 000 Report, vol. 16. Swedish Radiation Protection Authority (SSI), Tallinn.
Przylibski, T.A., 1999. Radon concentration changes in the air of two caves in Poland. J. Environ. Radioactiv. 45, 81–94.
Przylibski, T.A., 2011. Shallow circulation groundwater – the main type of water containing hazardous radon concentration. Nat. Hazard. Earth Sys. 11, 1695–1703.
Reimann, C., Filzmoser, P., Garrett, R., Dutter, R., 2008. Statistical Data Analysis Explained: Applied Environmental Statistics with R. John Willey and Sons Ltd., England.
Righi, S., Bruzzi, L., 2006. Natural radioactivity and radon exhalation in building materials used in Italian dwellings. J. Environ. Radioactiv. 88, 158–170.
Smetanová, I., Holy, K., Müllerová, M., Poláškova, A., 2010. The effect of meteorological parameters on radon concentration in borehole air and water. J. Radioanal. Nucl. Ch 283, 101–109.
Sundal, A.V., Valen, V., Soldal, O., Strand, T., 2008. The influence of meteorological parameters on soil radon levels in permeable glacial sediments. Sci. Total Environ. 389, 418–428.
Szabó, Z., Völgyesi, P., Nagy, H.É., Szabó, C., Kis, Z., Csorba, O., 2013. Radioactivity of natural and artificial building materials – a comparative study. J. Environ. Radioactiv. 118, 64–74.
Szucs, A., Jordan, G., 1994. Analysis of sampling frequency in groundwater quality monitoring systems: a case study. Water Sci. Technol. 30, 73–78.
Tanner, A.B., 1980. Radon migration in the ground: supplementary review. In: Gesell, T.F., Lowder, W.M. (Eds.), Proc. Natural Radiation Environment III, Conf-780422, US Dept. of Commerce, National Technical Information Service, Springfield, VA, p. 5.
Tukey, J.W., 1977. Exploratory Data Analysis. Addison-Wesley.
Velleman, P.F., Hoaglin, D.C., 1981. Applications, Basics and Computing of Exploratory Data Analysis. Duxbury Press, Boston.
Winkler, R., Ruckerbauer, F., Bunzl, K., 2001. Radon concentration in soil gas: a comparison of the variability resulting from different methods, spatial heterogeneity and seasonal fluctuations. Sci. Total Environ. 272, 273–282.
Zafrir, H., Barbosa, S.M., Malik, U., 2012. Differentiation between the effect of temperature and pressure on radon within the subsurface geological media. Radiat. Meas.. Article in press.